THE JOURNAL OF BIOLOGICAL CHEMISTRY VOL. 280, NO. 49, pp. 40474–40480, December 9, 2005
© 2005 by The American Society for Biochemistry and Molecular Biology, Inc. Printed in the U.S.A.

Functions of Early (AP-2) and Late (AIP1/ALIX) Endocytic Proteins in Equine Infectious Anemia Virus Budding*

Received for publication, August 24, 2005, and in revised form, October 6, 2005 Published, JBC Papers in Press, October 7, 2005, DOI 10.1074/jbc.M509317200

Chaoping Chen[‡], Olivier Vincent[§1], Jing Jin[‡], Ora A. Weisz[¶‖], and Ronald C. Montelaro[‡2]

From the Departments of [‡]Molecular Genetics and Biochemistry, [¶]Cell Biology and Physiology, and [‖]Medicine, Renal-Electrolyte Division, University of Pittsburgh School of Medicine, Pittsburgh, Pennsylvania 15261 and the [§]Departamento de Microbiologia Molecular, Centro de Investigaciones Biologicas del Consejo Superior de Investigaciones Cientificas, Madrid 28006, Spain

The proline-rich L domains of human immunodeficiency virus 1 (HIV-1) and other retroviruses interact with late endocytic proteins during virion assembly and budding. In contrast, the YPDL L domain of equine infectious anemia virus (EIAV) is apparently unique in its reported ability to interact both with the μ2 subunit of the AP-2 adaptor protein complex and with ALG-2-interacting protein 1 (AIP1/Alix) protein factors involved in early and late endosome formation, respectively. To define further the mechanisms by which EIAV adapts vesicle trafficking machinery to facilitate virion production, we have examined the specificity of EIAV p9 binding to endocytic factors and the effects on virion production of alterations in early and late endocytic protein expression. The results of these studies demonstrated that (i) an ~300-residue region of AIP1/Alix-(409–715) was sufficient for binding to the EIAV YPDL motif; (ii) overexpression of AIP1/Alix or AP-2 μ2 subunit specifically inhibited YPDL-mediated EIAV budding; (iii) virion budding from a replication-competent EIAV variant with its L domain replaced by the HIV PTAP sequence was inhibited by wild type or mutant μ2 to a level similar to that observed when a dominant-negative mutant of Tsg101 was expressed; and (iv) overexpression or siRNA silencing of AIP1/Alix and AP-2 revealed additive suppression of YPDL-mediated EIAV budding. Taken together, these results indicated that both early and late endocytic proteins facilitate EIAV production mediated by either YPDL or PTAP L domains, suggesting a comprehensive involvement of endocytic factors in retroviral assembly and budding that can be accessed by distinct L domain specificities.

Equine infectious anemia virus (EIAV)[2] is a member of the lentivirus subfamily of retroviruses, which also includes human immunodeficiency virus 1 (HIV-1). The EIAV genome is the simplest among the lentivirus family and encodes three major structural proteins (Gag, Pol, and Env) along with three accessory gene products (Tat, Rev, S2). Like all retroviruses, EIAV Gag protein is synthesized as a polyprotein that upon virion maturation is processed by virus-encoded protease to yield four major structural proteins: matrix, capsid, nucleocapsid, and p9 protein. All four structural proteins of Gag polyprotein play critical and distinctive roles in retrovirus assembly and budding. Matrix proteins direct targeting of Gag polyproteins to cell membranes for viral assembly and budding (1, 2). Both capsid and nucleocapsid have been shown to mediate Gag-Gag interactions during viral assembly, with capsid responsible for the dimerization of homologous Gag polyproteins (3, 4) and nucleocapsid essential for multimerization of Gag molecules (5, 6). The EIAV p9 protein contains a YPDL late (L) domain that is critical for virion release during the late stage of virus budding. Proline-rich L domains such as PTAP and PPPY with similar functions have also been identified from HIV-1, Rous sarcoma virus, and a variety of other enveloped viruses (7).

L domains appear to serve as docking sites to recruit cellular factors, providing essential functions for virion release. The HIV-1 PTAP motif specifically interacts with the N terminus of tumor suppression gene 101 products (Tsg101), an essential component of the ESCRT I complex responsible for multivesicular body (MVB) formation (8, 9). The PPPY motif binds to ubiquitin ligase Nedd4 (10, 11). Interestingly, the EIAV YPDL motif has been shown to interact with two cellular proteins, ALG-2-interacting-protein-1 (AIP1/Alix) (AIP1 is used hereinafter) (12, 13) and the μ2 subunit of the AP-2 adaptor protein complex (14). Although these L domains appear to interact with different cellular proteins, certain functional interchangeability was previously reported. For example, both PTAP and PPPY motifs can substitute for the YPDL domain to support EIAV replication (15). The PTAP function for HIV-1 budding and replication, however, can be replaced by the PPPY but not the YPDL motif (16). These observations indicate that retroviruses, along with other enveloped viruses, may have evolved different L domains to exploit redundant cellular endocytic machineries to achieve virus budding and release.

The L domain-interacting cellular proteins identified to date are endocytic components associated with the formation of either early endosomes (*e.g.* ubiquitin ligase, AP-2) or late MVBs (*e.g.* Tsg101, AIP1). Although it is currently assumed that MVBs play a central role in retrovirus budding, it remains uncertain whether and how components of other endosomal vesicles, including early endosomes, contribute to retroviral budding. It is reported that HLTV-1 Gag polyproteins interact first with Nedd4.1 at the plasma membrane and then with Tsg101 in late endosomes/MVB, suggesting a successive assembly and budding process through the endocytic pathway (17, 18). However, neither early nor late endosomes are optimally evolved for viral assembly and release. For example, the formation of early endosomes is topologically opposite that of viral budding, whereas budding into late endosome is topologically correct but imposes subsequent obstacles to virion release from infected cells. Therefore, it remains to be determined whether and how retroviruses combine and/or integrate early and late endosomal machinery to facilitate virion assembly and budding. In the light of

* This work was supported in part by National Institutes of Health Grant 2RO1 CA49296 (to R. C. M.), National Institutes of Health postdoctoral training Grant T32 AI49820 (to C. C.), and Comision Interministerial de Ciencia y Tecnología Grant BIO2002-00803 (to O. V.). The costs of publication of this article were defrayed in part by the payment of page charges. This article must therefore be hereby marked "*advertisement*" in accordance with 18 U.S.C. Section 1734 solely to indicate this fact.
[1] Supported by the Ramón y Cajal Program (Ministerio de Ciencia y Tecnología, Spain).
[2] To whom correspondence should be addressed: Dept. of Molecular Genetics and Biochemistry, University of Pittsburgh School of Medicine, W1144 Biomedical Science Tower, Pittsburgh, PA 15261. Tel.: 412-648-8869; Fax: 412-383-8859; E-mail: rmont@pitt.edu.
[2] The abbreviations used are: EIAV, equine infectious anemia virus; HIV-1, human immunodeficiency virus 1; AP-2, activator protein-2; AIP1, ALG-2-interacting-protein 1; Alix, ALG-2-interacting-protein x; MVB, multivesicular body; GST, glutathione *S*-transferase; HA, hemagglutinin; siRNA, small interfering RNA; shRNA, small hairpin RNA.; RT, reverse transcription

previous observations that the EIAV YPDL L domain interacts with both AP-2 and AIP1 in different model systems, the current study was designed to examine the specificity of EIAV p9 binding to early and late endocytic factors and the effects of alterations in early and late endocytic protein expression on virion production. The results of these studies demonstrated a previously unrecognized involvement of both early and late endocytic machinery in EIAV virion assembly and budding, whether accessed by YPDL or PTAP L domains.

EXPERIMENTAL PROCEDURES

Plasmids and DNA Mutagenesis—Construction of CMV_{uk} proviral EIAV and the CMV_{uk} PTAP derivative was described previously (15). The plasmid encoding LexA-*p9 was constructed by inserting the *p9 fragment of a GST-*p9 construct (14) in the polylinker site of pLexA-(1–202)+PL (19). Full-length AIP1, $AIP1_{372-869}$, or $AIP1_{409-715}$ were PCR-amplified and inserted into the Gal4 activation domain expression vector pACTII (Clontech). Plasmids encoding GST-*p2b, GST-*p6, and GST-*p9 or mutant derivatives were described previously (14) and confirmed by DNA sequencing. The gene segment encoding AIP1 residues 409–715 was PCR-amplified and inserted in-frame into pET32c(+) (Novagen, San Diego, CA). Plasmids expressing $Tsg101_{1-204}$ were obtained from Dr. Eric Freed (NIAID, National Institutes of Health, Frederick, MD) with the permission of Dr. Zijie Sun (Stanford University School of Medicine). Vectors expressing HA-tagged full-length and truncated AIP1/Alix proteins were generated by inserting PCR-amplified fragment into pCMV-HA (Clontech). pCDNA3.1 derivative expressing HA-tagged wild type $\mu 2$ was a gift from Dr. Alexander Sorkin (University of Colorado Health Science Center), and the mutant $\mu 2_{DW}$ was generated using standard molecular cloning protocols. pSilencer plasmid was purchased from Ambion (Austin, TX), and sequences of AIP1 (5′-gctcaagatggtgtgataa-3′) or (5′-gatcaagcgcatggcattcat-3′) were selected to generate pSilencer constructs that produce small hairpin RNA (shRNA), which was then spontaneously processed *in vivo* into siRNA.

Cell Culture and Transfection—COS-1 cells were cultured in minimum essential medium as described previously (20). HeLa and 293T cells were cultured in Dulbecco's modified Eagle's medium (Invitrogen) containing 10% fetal bovine serum. GenePorter II (Gene Therapy Systems, San Diego, CA) or FuGENE 6 (Roche Diagnostics) was used to transfect cells according to the manufacturer's recommendation. SiRNA duplexes were synthesized *in vitro* and transfected into HeLa cells using GeneEraser™ (Stratagene, La Jolla, CA).

Yeast Two-hybrid Analysis—The *Saccharomyces cerevisiae* strain used for two-hybrid studies was CTY10.5d (*Mat***a** *ade2-101 his3-Δ200leu2-Δ1 trp1-Δ901gal4 gal80 URA3::lexAop-lacZ*). Yeast were grown in synthetic dextrose medium lacking appropriate supplements to maintain selection for plasmids. β-Galactosidase activity was assayed on permeabilized cells grown to mid-log phase in the selective synthetic dextrose medium and expressed in Miller units. Yeast protein extracts for immunoblot analysis were prepared as described previously (21) and analyzed by immunoblotting with a monoclonal anti-HA antibody (Roche Diagnostics).

GST Pull-down Assays—GST fusion proteins and N-terminally His-tagged $AIP1_{409-715}$ were expressed from *Escherichia coli* BL21(DE3)pLysS (Novagen, Madison, WI). Bacterial extracts were prepared in STE buffer (10 mM Tris-HCl, pH 8.0, 150 mM NaCl, 1 mM EDTA) + 1% (v/v) Triton X-100, 5 mM dithiothreitol, and Complete™ protease inhibitor mixture (Roche Diagnostics), as described previously (22). Extracts containing GST-*p2b, GST-*p6, and GST-*p9 or mutant derivatives were incubated with glutathione-Sepharose 4B beads (Amersham Biosciences) at 4 °C for 1 h. After six washes with 1 ml of buffer STE/1% Triton X-100, beads with bound proteins were incubated with bacterial extract (500 μl) containing His-tagged $AIP1_{409-715}$ at 4 °C for 1 h. After six washes with STE/1% Triton X-100, beads were boiled in sample buffer, and proteins were separated by 10% polyacrylamide SDS-PAGE. Bound His-tagged $AIP1_{409-715}$ was detected by Western analysis with an anti-His tag antibody and enhanced chemiluminescence with reagents from Amersham Biosciences.

Reverse Transcriptase (RT) and Western Blotting Assays—To measure virion production, culture medium collected from 24 to 48 h after transfection was clarified of cell debris by low speed centrifugation and then centrifuged at 20,800 × *g* for 3 h at 4 °C to pellet virions. Virion pellets were resuspended in 50 μl of phosphate-buffered saline, and 10-μl samples were assayed in RT assays as described previously (20).

To examine EIAV-specific protein content in transfected cells and pelleted virions, total cell lysates prepared as described previously (20) and pelleted virions were resolved by electrophoresis through 4–15% gradient gels (Bio-Rad) and immunoblotted using a reference immune serum from a field-infected horse (20). Horseradish peroxidase-conjugated goat anti-horse IgG $F(ab')_2$ (Jackson ImmunoResearch, West Grove, PA) was used as secondary antibody. The immunoblots were developed by incubation with SuperSignal West Pico chemiluminescent substrate (Pierce). Horseradish peroxidase-conjugated high affinity anti-HA antibody (Roche Applied Science) was used to specifically detect HA-tagged proteins.

RESULTS

Interaction between AIP1 and EIAV p9 Proteins—Interaction between AIP1 and EIAV p9 was previously demonstrated using yeast two-hybrid and GST pull-down assays (12, 13, 23). To serve as a starting point for a comprehensive comparison, we initially examined the p9-AIP1 interaction using similar approaches. We previously demonstrated interaction between the $\mu 2$ subunit of the AP-2 adaptor protein complex and EIAV p9 using GST pull-down assay (24). In that study, a recombinant protein containing only the N-terminal 30 amino acids of EIAV p9 was fused to GST, in contrast to the full-length p9 protein (51 residues) used in studies of p9-AIP1 binding (12, 13, 23). Therefore, we performed p9-AIP1 binding assays using the N terminus of p9 (designated as *p9) in this study. Fig. 1 summarizes the yeast two-hybrid results using *p9 as bait to examine binding activities of full-length and two truncated AIP1 proteins. Full-length AIP1 bound to *p9 as expected (Fig. 1*A*), and interaction of two truncated fragments ($AIP1_{372-869}$ and $AIP1_{409-715}$) with *p9 was also detected. The stronger interaction of full-length AIP1 was not due to higher expression of the fusion protein as shown by Western blot analysis (Fig. 1*B*). The observed binding properties are consistent with previous studies showing that both the N terminus (1–175) and the C-terminal proline-rich domain (717–869) of AIP1 are not required for this interaction (12, 13, 23). Additionally, the current studies further defined the p9 binding domain of AIP1 to residues 409–715. It is interesting to note that the EIAV p9 binding domain of AIP1 (residues 409–715) does not contain the PSAP motif ($AIP1_{717-720}$) involved in interaction with Tsg101 (13).

To compare the binding properties of AIP1 proteins and the $\mu 2$ subunit in parallel, we performed GST pull-down assays using GST-*p9 and the $AIP1_{409-715}$ construct. Our data revealed that similar levels of GST fusion protein were produced from each construct (Fig. 2*A*) and that *p9 evidently bound to the $AIP1_{409-715}$. Single alanine substitutions in the EIAV L domain at residues Tyr-23, Pro-24, or Leu-26 abolished detectable $AIP1_{409-715}$ binding, suggesting their critical role for AIP1 interaction, whereas mutation of D25A reduced $AIP1_{409-715}$ binding by about

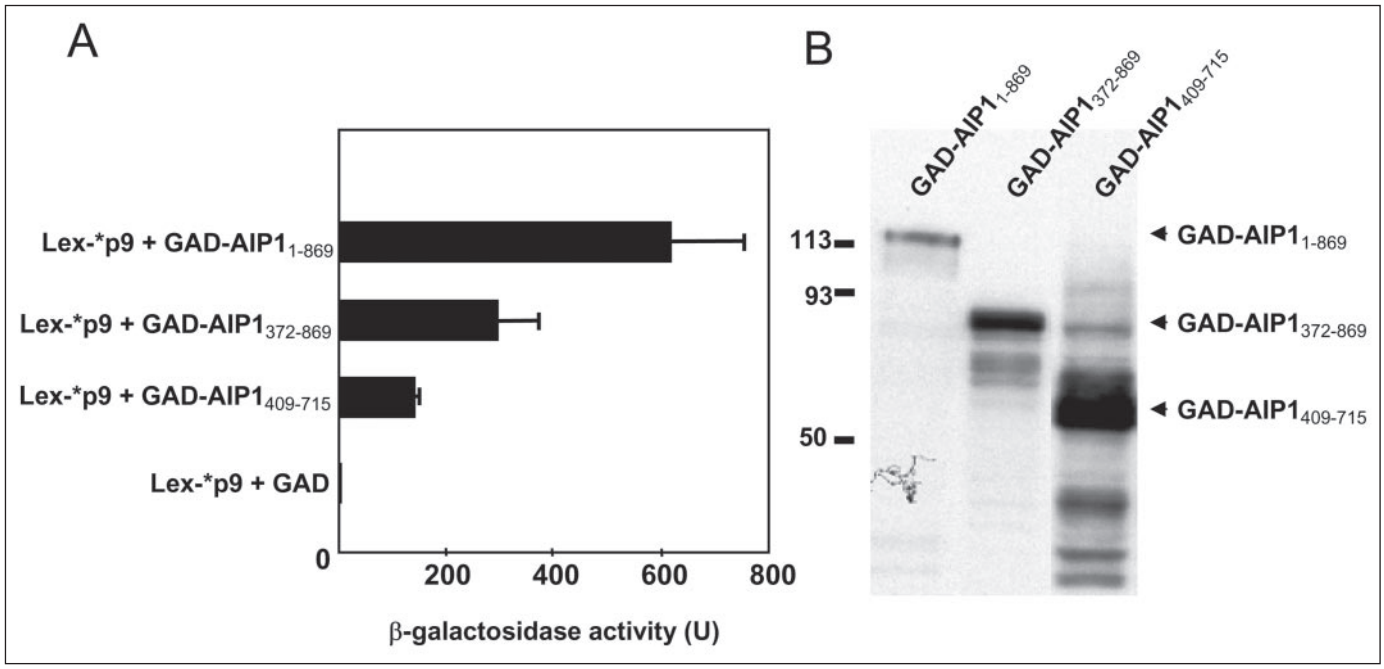

FIGURE 1. **Characterization of EIAV p9 interaction with AIP1 using the yeast two-hybrid system.** The yeast strain CTY10-5d was used and fusion proteins were expressed from pLexA-(1–202)+PL and pACTII derivatives. *A*, GAD-AIP1 fusions contain the indicated AIP1 residues. Interaction of p9 with AIP1 and its truncated forms was reflected in β-galactosidase activity (average of four transformants with standard deviation). *B*, Western analysis of protein extracts from transformants expressing LexA-p9 and the indicated GAD-AIP1 protein fusions, which were detected with anti-HA antibodies. The positions of the different protein fusion proteins are indicated by *arrows*.

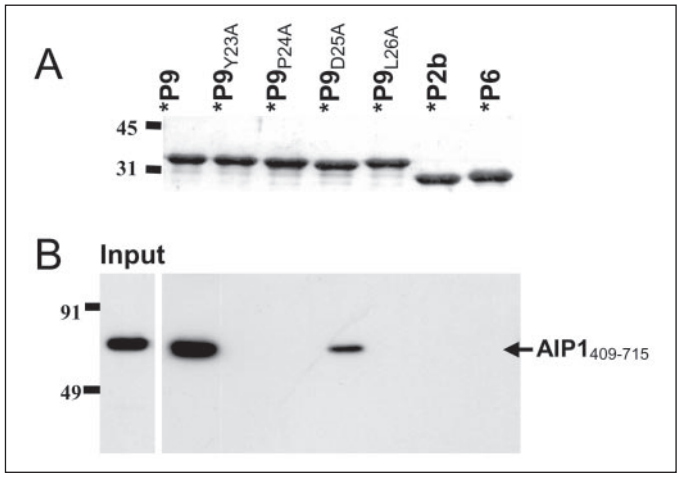

FIGURE 2. ***In vitro* binding of AIP1$_{409-715}$ to EIAV p9 and mutant derivatives.** *A*, GST fusions proteins bound to glutathione-Sepharose beads (one-half of the total) were separated by 10% SDS-PAGE and stained with Coomassie Blue. *B*, the remaining beads, loaded with GST-*p2b (SAPPPPYVGS), GST-*p6 (SRPEPTAPPEES), and GST-*p9 (SVPKNGKQGAQGRPQKQTFPIQQKSQHNKSVVQETPQTQNLYPDLSEIK) or mutant derivatives, were incubated with a bacterial extract containing His-tagged AIP1$_{409-715}$. After washing the beads, bound proteins were boiled in sample buffer, separated by SDS-PAGE, and analyzed by immunoblotting with anti-His tag antibody. The lane marked *Input* contains 2% of the bacterial extract used for binding experiments. Protein markers are in kDa.

70% when compared with *p9. The D25A substitution in p9 has previously been reported to have no effect on EIAV viral budding (24). Our data confirmed that the YPDL sequence is a critical determinant of AIP1-p9 interaction, consistent with other reports (12, 13, 23). Interestingly, the YPDL sequence specificity for AIP1 binding reported here is similar to that for p9 binding to μ2 that we described previously (24). The *p6 protein (SRPEPTAPPEES) did not bind to AIP1$_{409-715}$ as expected due to the absence of the p6 LYP motif responsible for AIP1 interaction in this construct. The observation that RSV *p2b failed to bind to AIP1$_{409-715}$ further confirmed the specificity of AIP1 interaction. Taken together, these data demonstrated that interaction of EIAV p9 and AIP1 is dependent on the p9 YPDL sequence and on a small region (residues 409–715) of the AIP1 protein. Thus, it appeared that *in vitro*, both AIP1 and μ2 equally interact with EIAV p9 protein via the YPDL sequence, suggesting possible interactions with early and late endocytic proteins in infected cells.

Effects of AIP1 Proteins on EIAV Budding—Previous studies of AIP1 interaction with the YPDL sequence of EIAV p9 protein were performed using Gag expression vectors and not with full-length EIAV proviral constructs. To examine the functional role of AIP1-p9 interactions in virion production in the context of complete proviral expression, we co-transfected COS-1 cells with an EIAV proviral construct and AIP1 expression vectors. As a specificity control, we also included an expression vector encoding the N-terminal moiety of Tsg101$_{1-204}$ that contains the HIV-1 PTAP binding domain (25). As summarized in Fig. 3, EIAV production was reduced by 50–70% from cells expressing AIP1 proteins when compared with cells transfected with vector DNA (Fig. 3*A*). Various AIP1 proteins differed slightly in their inhibitory effect on EIAV budding, with the full-length AIP1 apparently the most potent inhibitor despite the relatively low levels of full-length AIP1 detected in transfected cells. Another interesting observation is that co-expression of Tsg101$_{1-204}$ reproducibly enhanced EIAV production by an average of 30–40% when compared with the vector control. Overexpression of AIP1 proteins and Tsg101$_{1-204}$ seemed not to significantly affect the steady state levels of EIAV-specific protein as shown in Fig. 3*B* (*upper panel*). Thus, these data demonstrated that EIAV budding mediated by the YPDL domain is specifically inhibited by AIP1 protein overexpression.

To further verify the specificity of the interactions observed above, we next examined the presence of HA-tagged AIP1 proteins in pelleted EIAV virions. Our data showed that all three AIP1 proteins as well as Tsg101 were detected in pelleted virions (Fig. 3*B*, *lower panel*). To exclude the possibility that overexpression of these endocytic proteins results in their appearance in the pelletable fraction of the culture medium, we transfected COS-1 cells with the various endocytic protein

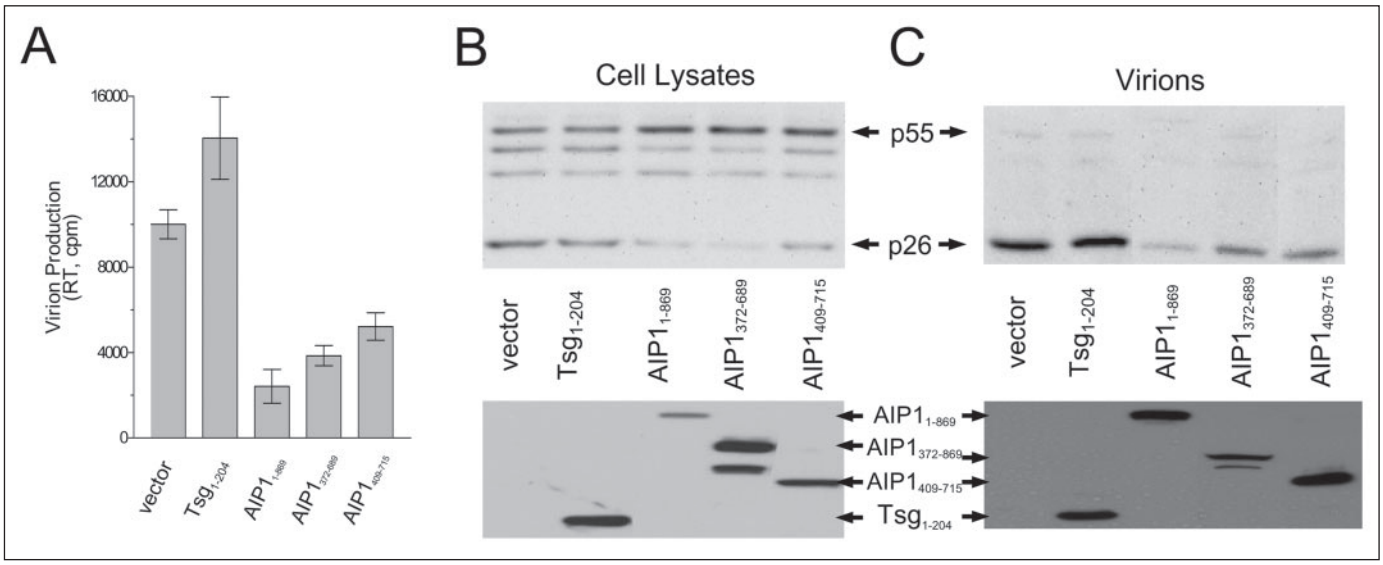

FIGURE 3. **Effect of overexpressed AIP1/Alix proteins on EIAV budding.** COS-1 cells grown on 6-well plates were co-transfected with CMV_{uk} proviral DNA and plasmids encoding for the indicated proteins at a 1:3 mass ratio with GenePorterII. Culture medium from 24 to 48 h after transfection was collected and centrifuged to pellet virions. *A*, RT activity of 10 μl of resuspended virions was assayed to quantify virion production. Data represent means ± ranges for duplicate samples from one of two independent experiments. *B*, at 48 h after transfection, cell lysates were prepared to examine cell-associated EIAV-specific viral proteins (*upper panel*) and expression of HA-tagged Tsg101 or AIP1 proteins (*lower panel*). *C*, resuspended virions were examined for content of the major viral structural protein p26 (*upper*) and of HA-tagged proteins (*lower*).

expression vectors in the absence of EIAV proviral DNA and centrifuged the culture medium under conditions used to pellet EIAV virions. No AIP1 or Tsg101 could be detected by immunoblotting in these control pelleted preparations in the absence of virion production (data not shown). Therefore, our results further confirmed specific incorporation of AIP1 into EIAV virions. The incorporation of Tsg101 into EIAV virions that we observed also suggested its involvement in EIAV budding, perhaps through indirect interactions mediated by AIP1-Tsg101 interaction (13).

Effects of AIP1 and μ2 Expression on EIAV Budding—Results from the preceding experiments and previous reports have confirmed that both AIP1 and μ2 bind to the YPDL sequence of EIAV p9 protein in GST pull-down assays and that overexpression of AIP1 inhibits EIAV budding from transfected COS-1 cells. We next compared the roles of AIP1 and μ2 in EIAV budding using wild type EIAV ($CMVuk_{YPDL}$) and a mutant EIAV ($CMVuk_{PTAP}$) with its YPDL motif replaced by the HIV-1-derived PTAP motif. AIP1 and μ2 inhibited EIAV budding by 60 and 50%, respectively, as measured by pelleted virion-associated RT activity (Fig. 4*A*). The specificity of μ2 inhibition was further confirmed by the observation that overexpression of a mutant μ2 ($\mu 2_{DW}$) that is unable to bind to EIAV p9 protein had no significant effect on EIAV production (Fig. 4*A*). Thus, both AIP1 and μ2 contributed to EIAV budding.

Overexpression of $Tsg101_{1-204}$ enhanced CMV_{uk}(YPDL) budding by about 30% (Fig. 4*A*) as observed in Fig. 3*A*, and budding of CMV_{uk}(PTAP) was inhibited about 55% by overexpressed $Tsg101_{1-204}$ as expected (Fig. 4*B*). These two proviral constructs only differ from each other in the specificity of the L domain sequences, and both are previously demonstrated to be replication-competent (15). Our data indicated that Tsg101 is involved in both PTAP- and YPDL-mediated retrovirus budding but probably through different interaction mechanisms. Interestingly, expression of both wild type and mutant μ2 reduced CMV_{uk}(PTAP) budding by about 80% (Fig. 4*B*), indicating that the AP-2 adaptor protein complex might also participate in PTAP-mediated budding, although direct interaction with the PTAP motif may not be required.

The involvement of both early and late endocytic proteins in retrovirus budding is also supported by the observation that these proteins could be co-pelleted with the EIAV virion (Fig. 4, *C* and *D*). It appeared that there was more $Tsg101_{1-204}$ and $AIP1_{409-715}$ incorporated into pelleted EIAV virions when compared with the levels of μ2 subunit. There are several possible explanations for the observed differences. Although all proteins were detected via their HA epitope tags, the positions of these tags differ (N-terminal for Tsg101 and AIP1, internal for μ2), possibly affecting the level of antibody reactivity of each protein to the anti-HA conjugate used in our immunoblots. If equal reactivity is assumed, different incorporation of these proteins might be the result of varied levels of these proteins expressed in the transfected cells (cell lysate data not shown). In particular, AP-2 expression is under such a tight regulation that loss of one subunit leads to complete depletion of AP-2 (26), and robust expression of AP-2 complex is difficult to achieve by overexpressing only one subunit of the complex. Taken together, our results demonstrated that both AIP1 and the μ2 subunit of AP-2 contribute to YPDL-mediated EIAV budding and that AP-2 also participates in PTAP-mediated budding.

Combined Effect of AIP1 and μ2 Overexpression on EIAV Budding—As both $AIP1_{409-715}$ and μ2 overexpression inhibited EIAV budding, we sought to determine whether they function independently or in cooperation. For this purpose, we individually titrated the minimum amounts of $AIP1_{409-715}$ or μ2 expression vector for detectable inhibitory effect (data not shown). Based on these assays, we cotransfected 293T cells using 0.8 μg of μ2 and 0.2 μg of $AIP1_{409-715}$, individually or in combination, whereas keeping the total amount of DNA constant with blank vector plus EIAV proviral DNA. Virions released into the culture medium during the period from 24 to 48 h after transfection were pelleted, and RT activity associated with the resuspended pellet was measured to quantify EIAV budding (Fig. 5). Co-expression of μ2 and $AIP1_{409-715}$ inhibited EIAV budding more than either protein expressed individually (80% *versus* 40 and 50% inhibition, respectively), indicating an additive effect of AIP1 and μ2 and further supporting the concept that both AIP1 and μ2 contribute to EIAV budding. To test whether the combined effect was cell type-dependent, we also carried out the same experiment in COS-1 cells and found similar results (Fig. 5*B*). Incorporation of $AIP1_{409-715}$ and μ2 was also detected in pelleted EIAV virions (Fig. 5*C*).

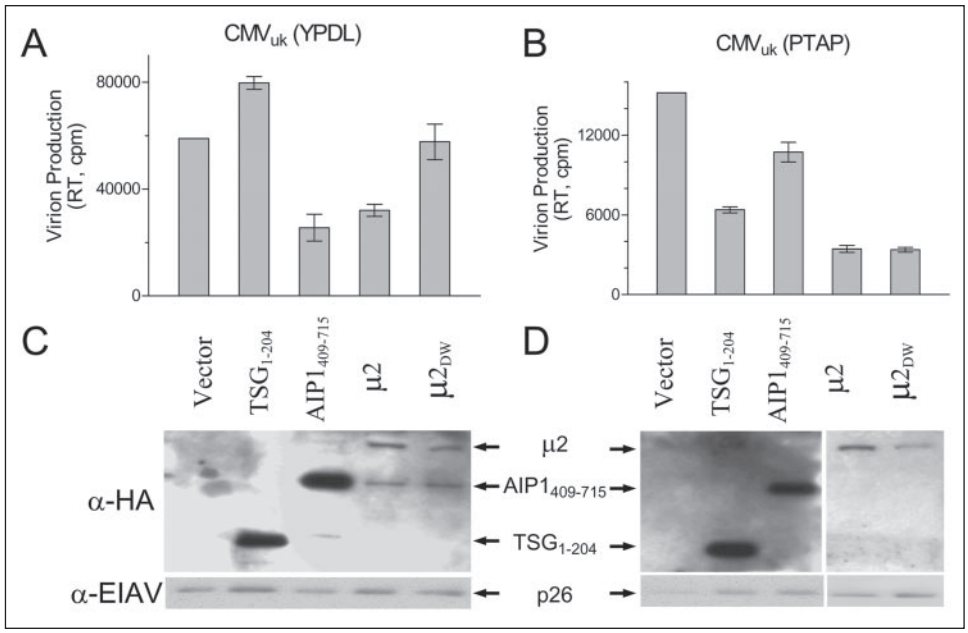

FIGURE 4. **Effect of individually overexpressed endocytic proteins on EIAV budding.** COS-1 cells grown on 6-well plates were transfected with CMV$_{uk}$(YPDL) (*A*) or CMV$_{uk}$ PTAP proviral DNA (*B*) along with plasmids encoding for the indicated proteins at a 1:2 mass ratio using FuGENE 6. Culture medium from 24 to 48 h after transfection was collected. RT activity of pelleted virions was assayed to represent virion production. Data represent means ± ranges for duplicate samples from one of two independent experiments. Approximately equal amounts of resuspended virions normalized by RT activity were also subjected to Western blot to examine the content of HA-tagged endocytic proteins associated with the pelleted virions produced from CMV$_{uk}$(YPDL) (*C*) or CMV$_{uk}$(PTAP) (*D*) transfection.

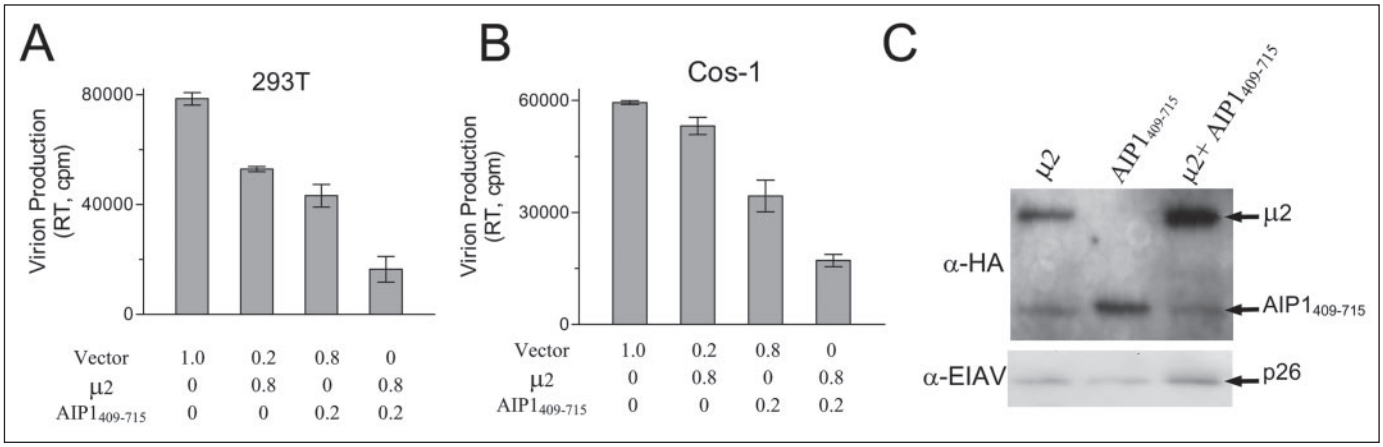

FIGURE 5. **Additive effect of overexpressed μ2 and AIP1$_{409-712}$ proteins on EIAV budding.** 293T (*A*) and COS-1 (*B*) cells grown on 6-well plates were co-transfected with 1 μg of CMV$_{uk}$ proviral DNA and a total of 1 μg of indicated plasmids using FuGENE 6. Culture medium from 24 to 48 h after transfection was collected to pellet virions. RT activity of 10 μl of resuspended virions was measured to represent virion production. Data represent means ± ranges for duplicate samples from one of three independent experiments. *C*, approximately equal amounts of resuspended virions produced from the transfected COS-1 cells normalized by RT activity were also examined for the content of HA-tagged proteins.

siRNA and shRNA Silencing of μ2 and AIP1 on EIAV Budding—It has been cautioned that overexpression of certain proteins might nonspecifically affect global cellular functions rather than specifically disturbing the precise cellular pathway under investigation. To complement our overexpression study on the roles of μ2 and AIP1 in EIAV budding, we examined the effects of μ2 and AIP1 down-regulation on EIAV budding. Fraile-Ramos *et al.* (26) previously tested specific siRNA sequences against the μ2 subunit of AP-2 and demonstrated an average 50% reduction in μ2 expression in HeLa cells at 48 h after transfection. Based on the same siRNA sequence, we generated a pSilencer-derived DNA construct that produces small hairpin RNA (shRNAμ2) upon transfection, which is spontaneously processed into siRNA in the transfected cells. The silencing effect of this construct on COS-1 cells cotransfected with HA-tagged μ2 was examined (Fig. 6*A*). Consistent with the results of Fraile-Ramos *et al.* (26), shRNAμ2 reduced μ2 expression by about 50% at 48 h after transfection. To knock down AIP1 expression, we cloned several sequences targeting various regions of AIP1 into the pSilencer vector and identified a specific sequence (5′-gctcaagatggtgtgataa-3′) to achieve efficient silencing (Fig. 6*B*). At 48 h after co-transfection, expression of full-length AIP1 was reduced by about 80% and expression of AIP1$_{409-715}$ was reduced by about 70%, respectively.

Our results revealed that 70–80% of AIP1 silencing could be achieved by shRNA$_{AIP1,}$ but only about 50% of μ2 silencing was observed using either siRNA or shRNA at 48 h after transfection. The long half-life of μ2 subunit (~24 h) (27) might partially account for the relative inefficiency of knockdown procedures. Therefore, to more rigorously suppress AP-2 expression, assays at later time points (72–96 h after transfection) or two consecutive transfections were used to achieve higher levels of μ2 silencing (28). We therefore designed our experiments to first transfect 293T cells with siRNA duplex at day 0, and at day 2, cells were split, reseeded, and incubated for ~12 h prior to transfection using the EIAV proviral DNA with or without pSilencer vectors encoding the specific shRNA. RT activity in culture medium collected from 24 to 48 h after the second transfection was quantitated as a measure of EIAV budding. In Fig. 6*C*, we first transfected 293T cells with increasing concentrations of μ2 siRNA and used only EIAV proviral DNA during the second transfection. Under these conditions, EIAV budding was inhib-

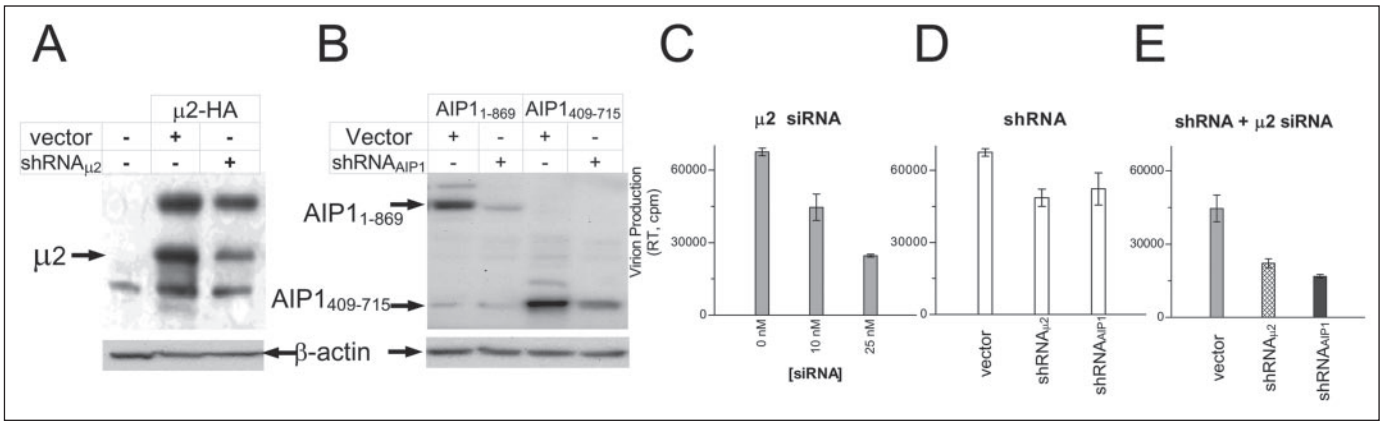

FIGURE 6. **Effect of siRNA and shRNA targeting $\mu 2$ and AIP1$_{409-715}$ on EIAV budding.** An siRNA sequence known to down-regulate $\mu 2$ expression (26) was used to generate pSilencer plasmid, denoted as shRNA$\mu 2$ here. A sequence (5′-gctcaagatggtgtgataa-3′) targeting to 1765–1783 nt downstream of AIP1 start codon was selected to make shRNAAIP1 pSilencer constructs. Down-regulation of $\mu 2$ (*A*) and AIP1 (*B*) was verified in COS-1 cells transfected with the indicated plasmids. Cell lysates were prepared at 48 h after transfection. Approximately equal amounts of cell lysates (normalized to β-actin) were immunoblotted with anti-HA antibody to detect $\mu 2$ and AIP1 proteins (*arrows*), respectively. *C*, the effect of $\mu 2$ siRNA on EIAV budding. 293T cells were transfected with siRNA targeting $\mu 2$ at the indicated concentrations. At 48 h after siRNA transfection, cells were split and reseeded and then incubated for another 12 h before they were transfected with EIAV proviral DNA. Culture medium from 24 to 48 h after the second transfection was collected to pellet virions, and RT activity of 10 μl of resuspended virions was measured to represent virion production. *D*, to evaluate the effect of shRNA alone on EIAV budding, 293T cells were transfected with the indicated constructs along with the EIAV proviral DNA. Virion production was measured as in *C* to quantify budding efficiency. *E*, the effects of siRNA and shRNA on EIAV budding. The same protocol used in *C* was followed except that 293T cells were first transfected with 10 nM siRNA targeting $\mu 2$, and EIAV proviral DNA along with the indicated shRNA constructs were included during the second transfection. Data represent means ± ranges for duplicate samples from one of two independent experiments.

ited by $\mu 2$ siRNA in a dose-dependent manner (Fig. 6*C*), *i.e.* no inhibition at 0 nM, 40% inhibition at 10 nM, and 60% inhibition at 25 nM $\mu 2$ siRNA. To assay the effect of the specific shRNA encoded by the pSilencers, we mock-transfected the 293T cells with the GeneEraser^{TM}. Following splitting and reseeding of the cells, we transfected them with EIAV proviral DNA along with the shRNA constructs. Our results in Fig. 6*D* showed that EIAV budding was reduced by about 15–20% by shRNA$_{\mu 2}$ and shRNA$_{AIP1}$, respectively, indicating that the shRNAs we generated affect EIAV budding as expected. In another experiment (Fig. 6*E*), 293T cells were first transfected with 10 nM $\mu 2$ siRNA and then transfected with EIAV proviral DNA and pSilencer constructs at 60 h after the first transfection. Expression of shRNA$_{\mu 2}$ further reduced EIAV production by about 50% and shRNA$_{AIP1}$ by about 60%, respectively. The inhibitory effect was cumulative for $\mu 2$ and AIP1 down-regulation, further confirming that both $\mu 2$ and AIP1 are involved in EIAV budding.

DISCUSSION

It has become increasingly appreciated that retroviruses have evolved to adapt various host cellular machinery for their replication, and the number of identified cellular factors that interact with viral proteins is rapidly increasing (7, 29–31). Recently, cellular proteins that specifically bind to retrovirus L domains have been extensively characterized (9, 10, 23, 24), providing strong evidence to link retrovirus budding with vesicular trafficking. However, the detailed molecular and cellular mechanisms that underlie the adaptation of endocytic proteins by retroviruses to facilitate budding remain to be illustrated.

In the current study, we compared the functions of the $\mu 2$ subunit of AP-2 and AIP1 in EIAV budding using complementary approaches. Our results revealed that disruption of $\mu 2$ or AIP1 expression, either up-regulation by transient transfection or down-regulation by siRNA silencing, reduced EIAV budding from cells cotransfected with an EIAV proviral construct. Furthermore, the effects of $\mu 2$ and AIP1 were cumulative, if not synergistic, as overexpression or knockdown of both resulted in more potent inhibition than that observed for either individual protein. Interestingly, our data demonstrated that HIV-1 PTAP L domain-mediated budding was also inhibited when $\mu 2$ subunit was overexpressed in the same cells. Therefore, the current report has provided evidence for a contribution of the AP-2 adaptor protein complex in both PTAP- and YPDL-mediated budding, in addition to the previously reported role of AIP1 in this process.

The $\mu 2$ subunit of AP-2 is a critical component for the formation of early endosomes, and identification of its interaction with the EIAV L domain suggested the involvement of the early endocytic pathway in retrovirus budding (24). However, the precise role of early endocytic proteins in viral budding has been controversial as the topology of endocytosis is opposite to that of retrovirus budding. The past few years have seen a collection of evidence that AIP1, a cellular component involved in late endosome/MVB formation, interacts with the EIAV YPDL L domain and an LYP motif located downstream of the PTAP motif in HIV p6 (12, 13, 23). Along with the identification of Tsg101 (a component of the ESCRT I complex essential for MVB formation) as the binding partner of HIV PTAP motif, these results suggest that retroviruses can recruit late endocytic machinery for budding as both processes share the same topology. However, it remains unclear whether and how retroviruses bud into late endosomes before they exit host cells. The current results that both $\mu 2$ and AIP1 contribute to YPDL- and PTAP-mediated budding strongly indicated that retrovirus might actually combine both early and late endosomal machinery to facilitate budding. Consistent with this model, MLV Gag polyproteins have been shown to traffic between the plasma membrane and the late endosomes, although the functional significance of this trafficking remains to be defined (17). Here we have reported that PTAP-mediated budding is also sensitive to $\mu 2$ overexpression and that both wild type and mutant $\mu 2$ had similar effects on budding. These data indicated that the AP-2 adaptor protein complex might contribute to retrovirus budding via a general mechanism that remains to be defined. It is also worth noting that when the $\mu 2$ subunit was depleted using high concentrations of siRNA oligonucleotides (25 nM), no further reduction in EIAV budding was observed upon introduction of a second shRNA (shRNA$\mu 2$ or shRNA$_{AIP1}$) by transfection (data not shown). These observations indicated that adaptation of $\mu 2$ and AIP1 might be sequential such that complete blockade of one interaction abolishes the entire chain. Further characterizations of the apparently complex interactions between the Gag proteins of different retroviruses and endocytic proteins involved in assembly and budding can provide further insights into the exact role of the endocytic machin-

ery in Gag trafficking, assembly, and budding. In addition, the characterization of these critical Gag-endocytic protein interactions can provide new targets for the development of antiviral drugs.

REFERENCES

1. Bryant, M., and Ratner, L. (1990) *Proc. Natl. Acad. Sci. U. S. A.* **87,** 523–527
2. Spearman, P., Wang, J. J., Vander, H. N., and Ratner, L. (1994) *J. Virol.* **68,** 3232–3242
3. Gamble, T. R., Yoo, S., Vajdos, F. F., von Schwedler, U. K., Worthylake, D. K., Wang, H., McCutcheon, J. P., Sundquist, W. I., and Hill, C. P. (1997) *Science* **278,** 849–853
4. Franke, E. K., Yuan, H. E., Bossolt, K. L., Goff, S. P., and Luban, J. (1994) *J. Virol.* **68,** 5300–5305
5. Derdowski, A., Ding, L., and Spearman, P. (2004) *J. Virol.* **78,** 1230–1242
6. Zhang, Y., Qian, H., Love, Z., and Barklis, E. (1998) *J. Virol.* **72,** 1782–1789
7. Demirov, D. G., and Freed, E. O. (2004) *Virus Res.* **106,** 87–102
8. VerPlank, L., Bouamr, F., LaGrassa, T. J., Agresta, B., Kikonyogo, A., Leis, J., and Carter, C. A. (2001) *Proc. Natl. Acad. Sci. U. S. A.* **98,** 7724–7729
9. Garrus, J. E., von Schwedler, U. K., Pornillos, O. W., Morham, S. G., Zavitz, K. H., Wang, H. E., Wettstein, D. A., Stray, K. M., Cote, M., Rich, R. L., Myszka, D. G., and Sundquist, W. I. (2001) *Cell* **107,** 55–65
10. Kikonyogo, A., Bouamr, F., Vana, M. L., Xiang, Y., Aiyar, A., Carter, C. A., and Leis, J. (2001) *Proc. Natl. Acad. Sci. U. S. A.* **98,** 11199–11204
11. Irie, T., Licata, J. M., McGettigan, J. P., Schnell, M. J., and Harty, R. N. (2004) *J. Virol.* **78,** 2657–2665
12. Martin-Serrano, J., Yaravoy, A., Perez-Caballero, D., and Bieniasz, P. D. (2003) *Proc. Natl. Acad. Sci. U. S. A.* **100,** 12414–12419
13. von Schwedler, U. K., Stuchell, M., Muller, B., Ward, D. M., Chung, H. Y., Morita, E., Wang, H. E., Davis, T., He, G. P., Cimbora, D. M., Scott, A., Krausslich, H. G., Kaplan, J., Morham, S. G., and Sundquist, W. I. (2003) *Cell* **114,** 701–713
14. Puffer, B. A., Parent, L. J., Wills, J. W., and Montelaro, R. C. (1997) *J. Virol.* **71,** 6541–6546
15. Li, F., Chen, C., Puffer, B. A., and Montelaro, R. C. (2002) *J. Virol.* **76,** 1569–1577
16. Ott, D. E., Coren, L. V., Gagliardi, T. D., and Nagashima, K. (2005) *J. Virol.* **79,** 9038–9045
17. Segura-Morales, C., Pescia, C., Chatellard-Causse, C., Sadoul, R., Bertrand, E., and Basyuk, E. (2005) *J. Biol. Chem.* **280,** 27004–27012
18. Blot, V., Perugi, F., Gay, B., Prevost, M. C., Briant, L., Tangy, F., Abriel, H., Staub, O., Dokhelar, M. C., and Pique, C. (2004) *J. Cell Sci.* **117,** 2357–2367
19. Ruden, D. M., Ma, J., Li, Y., Wood, K., and Ptashne, M. (1991) *Nature* **350,** 250–252
20. Chen, C., Li, F., and Montelaro, R. C. (2001) *J. Virol.* **75,** 9762–9770
21. Vincent, O., and Carlson, M. (1999) *EMBO J.* **18,** 6672–6681
22. Vincent, O., Rainbow, L., Tilburn, J., Arst, H. N., Jr., and Penalva, M. A. (2003) *Mol. Cell. Biol.* **23,** 1647–1655
23. Strack, B., Calistri, A., Craig, S., Popova, E., and Gottlinger, H. G. (2003) *Cell* **114,** 689–699
24. Puffer, B. A., Watkins, S. C., and Montelaro, R. C. (1998) *J. Virol.* **72,** 10218–10221
25. Demirov, D. G., Ono, A., Orenstein, J. M., and Freed, E. O. (2002) *Proc. Natl. Acad. Sci. U. S. A.* **99,** 955–960
26. Fraile-Ramos, A., Kohout, T. A., Waldhoer, M., and Marsh, M. (2003) *Traffic* **4,** 243–253
27. Nesterov, A., Carter, R. E., Sorkina, T., Gill, G. N., and Sorkin, A. (1999) *EMBO J.* **18,** 2489–2499
28. Motley, A., Bright, N. A., Seaman, M. N., and Robinson, M. S. (2003) *J. Cell Biol.* **162,** 909–918
29. Li, F., and Wild, C. (2005) *Curr. Opin. Investig. Drugs* **6,** 148–154
30. Dong, X., Li, H., Derdowski, A., Ding, L., Burnett, A., Chen, X., Peters, T. R., Dermody, T. S., Woodruff, E., Wang, J. J., and Spearman, P. (2005) *Cell* **120,** 663–674
31. Alroy, I., Tuvia, S., Greener, T., Gordon, D., Barr, H. M., Taglicht, D., Mandil-Levin, R., Ben Avraham, D., Konforty, D., Nir, A., Levius, O., Bicoviski, V., Dori, M., Cohen, S., Yaar, L., Erez, O., Propheta-Meiran, O., Koskas, M., Caspi-Bachar, E., Alchanati, I., Sela-Brown, A., Moskowitz, H., Tessmer, U., Schubert, U., and Reiss, Y. (2005) *Proc. Natl. Acad. Sci. U. S. A.* **102,** 1478–1483